

# The Role of Nanoparticles on Topographic Cross-Talk in Electric Force Microscopy and Magnetic Force Microscopy

Marc Fuhrmann, Alexander Krivcov, Anna Musyanovych, Ronald Thoelen, and Hildegard Möbius\*

Topographic cross-talk is still an issue in magnetic force microscopy (MFM) as well as in electric force microscopy (EFM). Using interleave mode measurements, combining a first topographic scan with a second scan in a certain distance from the surface following the topography from the first scan, capacitive coupling effects occur while measuring nanoparticles. This article focuses on the influence of the dielectric constant of polystyrene nanoparticles in interleave mode MFM measurements. To investigate the contribution of the capacitive coupling effect to the signal, nonmagnetic polystyrene nanoparticles are investigated. The tip-substrate distance change above the nanoparticle leads to a positive phase shift in MFM signals. Simulations and fits to the experimental data allow the investigation of the influence of the dielectric constant of the nanoparticles on topographic effects in interleave mode measurements in general.

## 1. Introduction

Electric force microscopy (EFM) and magnetic force microscopy (MFM) have gained much interest to explore the electrical and magnetic properties of nanoparticles. Intensive research activities are going on to image surface potential variations, charge density, and dielectric constants of nanostructures and thin films with EFM.<sup>[1–4]</sup> The demand for magnetic nanoparticles for biomedical applications such as drug delivery, magnetic resonance imaging, cell separation, and hyperthermia motivates

the characterization of nanoparticles and nanocarriers loaded with magnetic nanoparticles by MFM.<sup>[5–10]</sup> Both methods, EFM and MFM, use the so-called interleave mode, a two-pass technique, combining a first tapping mode scan line at the sample's surface with a scan line at a defined height above the surface following the topography. Additionally, both methods deal with the capacitive force between tip and substrate. In EFM, the electrostatic tip/sample interaction is used to provide information of nanostructured materials.<sup>[4,11,12]</sup> In MFM, electrostatic forces can overlap the magnetic signals resulting in a misleading interpretation of measured MFM data.<sup>[13,14]</sup>


Measuring nanoparticles with MFM, a mirroring of the topography has been reported and discussed by capacitive coupling effects.<sup>[15–18]</sup> In our previous work, capacitive coupling in MFM was theoretically explained and experimentally proved to be due to the distance change in the interleave mode measuring above the nanoparticle leading to a reduction of the electric force and thus to topographic cross talk.<sup>[17,18]</sup> Yu et al. avoided these topographic effects by combining MFM with EFM compensating the contact potential difference by applying an appropriate tip bias.<sup>[13]</sup> In EFM, topographic cross talk has been observed and discussed as well.<sup>[12,19]</sup> Tevaarwerk et al. distinguished the electrical properties from topographic EFM signals for nonflat nanoscale samples by electrostatic simulations which account for sample topography.<sup>[19]</sup> Focus of this article is MFM measurements on polystyrene nanoparticles to be used as carriers for magnetic nanoparticles. To isolate the electrostatic contribution from the magnetic signal, unloaded polystyrene nanoparticles of different sizes are investigated. In contrast to EFM measurements, the only voltage in MFM inducing the electrostatic contribution is given by the contact potential difference between tip and substrate. But, all theoretical considerations in this study on the influence of capacitive coupling on MFM signals can be transferred to EFM interleave mode measurements on nanoparticles.

To model the tip-substrate capacitance, various models have been developed ranging from a parallel-plate capacitor geometry to models including the form of the tip, e.g., sphere model, the uniform charge line model, and the combination of the sphere model for the tip apex, the conical shape of the tip, and a rectangular cantilever.<sup>[1,2,20]</sup> These models differ in the power law describing the  $z$ -dependence of the force gradient acting on the tip. Experiments showed that depending on the tip-substrate

M. Fuhrmann, Dr. A. Krivcov, Prof. H. Möbius  
Department of Computer Sciences/Micro Systems Technology  
University of Applied Sciences Kaiserslautern  
Amerikastr. 1, 66482 Zweibrücken, Germany  
E-mail: Hildegard.Moebius@hs-kl.de

Dr. A. Musyanovych  
Nanoparticle Technology Department  
Fraunhofer IMM  
Carl-Zeiss-Str. 18-20, 55129 Mainz, Germany

Prof. R. Thoelen  
Institute for Materials Research  
Hasselt University  
Martelarenlaan 42, 3500 Hasselt, Belgium

 The ORCID identification number(s) for the author(s) of this article can be found under <https://doi.org/10.1002/pssa.201900828>.

© 2020 The Authors. Published by WILEY-VCH Verlag GmbH & Co. KGaA, Weinheim. This is an open access article under the terms of the Creative Commons Attribution License, which permits use, distribution and reproduction in any medium, provided the original work is properly cited.

DOI: 10.1002/pssa.201900828

distance, different power laws are needed as the interaction and therefore the contribution of tip apex, cone, and cantilever varies with the distance. Hudlet et al. developed an analytical derivation of the electric field of a truncated cone and a spherical tip apex in the following called the Hudlet model.<sup>[21]</sup> In this study, we compare the Hudlet model with a parabolic tip shape based on the tip radius determined by scanning electron microscopy (SEM) measurements.

The aim of this work is to theoretically discuss and experimentally prove the influence of the dielectric constant of nanoparticles of different diameter on the capacitive coupling effect occurring in MFM and EFM due to distance changes in interleave mode measurements above the nanoparticle.

## 2. Theory

### 2.1. Capacitive Coupling Effects in MFM on Nanoparticles

Capacitive coupling between tip and substrate leads to a positive phase shift in MFM measurements on nanoparticles due to the tip-substrate distance change in the interleave mode above the nanoparticles.<sup>[17]</sup> Figure 1 shows a sketch of a standard interleave measurement procedure.

The force gradient due to the electrostatic force measured beside the nanoparticle is larger than the force gradient measured above the nanoparticle leading in total to a positive phase shift

$$\begin{aligned} \Delta\phi_{el} &= -\frac{Q}{k} (F'(z+d) - F'(z)) \\ &= -\frac{Q}{k} \epsilon_0 \left( \frac{A}{(z+d)^3} (V_{CPD})^2 - \frac{A}{z^3} (V_{CPD})^2 \right) > 0 \end{aligned} \quad (1)$$

where  $F'$  is the force gradient acting on the tip during the MFM measurement,  $Q$  is the cantilever quality factor,  $k$  the spring constant,  $\epsilon_0$  is the vacuum dielectric constant,  $z$  is the lift height,  $d$  is the diameter of the nanoparticle,  $A$  is the area of the capacitor, and  $V_{CPD}$  is the contact potential difference between

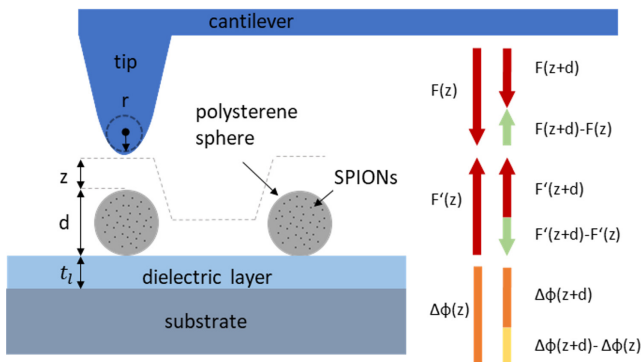


**Figure 1.** Sketch of interleave mode demonstrating the capacitive coupling effect due to distance change between tip and substrate above the nanoparticle and diagram of force, force gradient, and resulting phase shift (left arrows red: beside the nanoparticle; right arrows red: above the nanoparticle; green arrows: difference between forces, force gradient. Orange bar: negative phase shift beside and above the nanoparticle; yellow bar: resulting positive phase shift above the nanoparticle).

substrate and tip.<sup>[17]</sup> In this equation, the dielectric layer thickness  $t_l$  in Figure 1 is assumed to be zero. As Krivcov et al. investigated by Kelvin probe force microscopy (KPFM) measurements, the potential while measuring above a nanoparticle does not change and therefore  $V_{CPD}$  can be assumed to be constant.<sup>[18]</sup>

### 2.2. Estimation and Influence of the Effective Area of the Capacitor “Tip-Substrate”

Relevant for the capacitive coupling described earlier is the area of interaction between tip and substrate. In a simple model, the capacitor can be assumed to consist of two parallel circle plates with the effective area  $A_{eff}$ . In this study,  $A_{eff}$  is defined as the area of the capacitor responsible for the capacitive coupling. In reality,  $A_{eff}$  of the tip is a 3D surface depending on the form of the tip apex and the cone as well as on the tip-surface distance as shown in Figure 2.

As the value of the force gradient is a decreasing function of the tip-substrate distance, the effective area increases with increasing tip-substrate distance (Figure 2). Measuring nanoparticles in MFM, the distance change as shown in Figure 1 leads to an increasing effective area for the signals above the nanoparticles. To simulate the phase shifts due to capacitive coupling, the increasing effective area must be taken into account. Therefore, models are needed to calculate the effective area  $A_{eff}$ .

In the following, we compare the Hudlet model with a simple model assuming a parabolic tip shape.<sup>[1]</sup> 1) Hudlet et al. calculated the capacitive force between tip and substrate by considering the spherical contribution of the tip apex as well as the conical contribution of the tip.<sup>[1]</sup>

Assuming small cone angles  $\theta_0$ , the total force was determined to be

$$\begin{aligned} F_{tot} &= \pi \epsilon_0 V^2 \cdot \left( \frac{r_{tip}^2}{z \cdot (z + r_{tip})} \right) \\ &+ k^2 \cdot \left( \ln \frac{z + r_{tip}}{H} - 1 + \frac{r_{tip}}{\sin \theta_0 \cdot (z + r_{tip})} \right) \end{aligned} \quad (2)$$

with  $V$  is the voltage between tip and substrate,  $z$  is the lift height,  $H$  is the cone height, and  $\theta_0$  is the cone angle, with

$$k^2 = \frac{1}{[\ln(\tan(\theta_0/2))]^2} \quad (3)$$

The force gradient acting on the tip can be calculated as

$$\begin{aligned} F'_{tot} &= \pi \epsilon_0 V^2 \cdot \left( -\frac{r_{tip}^2 (2z + r_{tip})}{(z^2 + r_{tip} z)^2} \right) \\ &+ k^2 \cdot \left( \frac{1}{z + r_{tip}} - \frac{r_{tip}}{\sin(\theta_0) \cdot (z + r_{tip})^2} \right) \end{aligned} \quad (4)$$

The first part represents the contribution of the spherical tip apex and the second part represents the contribution of the cone.

These equations inherently contain the dependence of  $A_{eff}$  on the tip-substrate distance as the force is obtained by summing all contributions of forces of infinitesimal surfaces

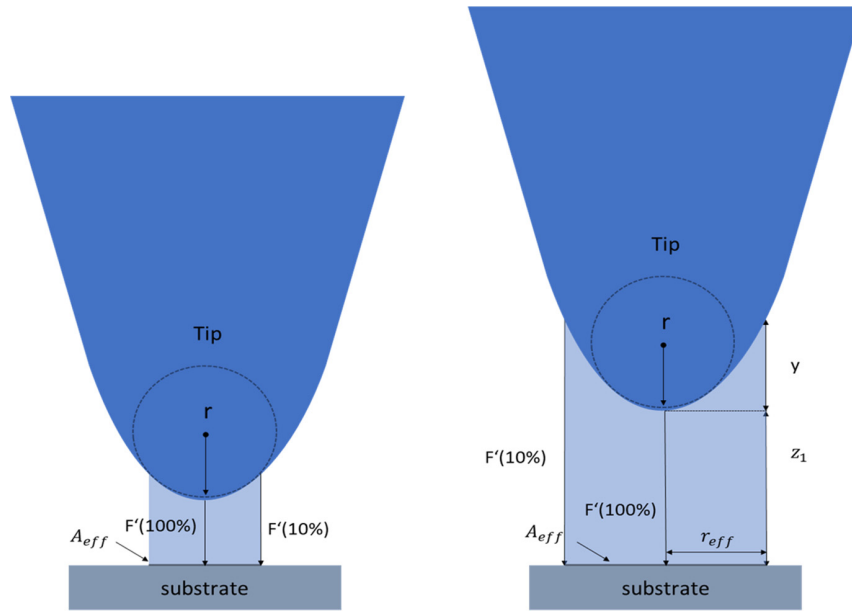


**Figure 2.** Effective area of the tip-substrate capacitor as a function of tip-substrate distance.

obtained by faceting the tip surface.<sup>[1]</sup> 2) Parabolic tip: Assuming a parabolic tip shape, the effective area can be calculated by defining an effective radius by the value of the force gradient falling below a certain value as shown in Figure 2. The value of the force gradient acting between tip and substrate at the effective radius falls below an assumed percentage of the force gradient value acting between tip and substrate at the middle of the tip  $F'(z_1, r_{\text{eff}}) \leq p \cdot F'(z_1, r=0)$ , where  $r_{\text{eff}}$  is the lateral distance to the middle of the tip and  $p$  is the percentage factor,  $z_1$  is the distance between tip and substrate. The tip shape is assumed to have a parabolic form  $y = \frac{r_{\text{tip}}^2}{r_{\text{tip}}^2} \cdot z^2$  with  $r_{\text{tip}}$  is the radius of the tip,  $r_{\text{eff}}$  is the effective radius. Therefore,  $r_{\text{eff}}$  can be calculated by

$$r_{\text{eff}} = \sqrt{\gamma \cdot r_{\text{tip}}} \quad (5)$$

Assuming  $F'$  in the middle of the tip to be 100% and the  $z$ -dependence of  $F'$  for constant  $A$ , the value of the force gradient will fall below  $p\%$  of  $F'$  at a tip-substrate distance of  $(z_1 + \gamma)$

$$\Rightarrow F'(z_1 + \gamma) = p \cdot F'(z_1) \quad (6)$$

$$\Rightarrow \frac{\epsilon_0 A}{(z_1 + \gamma)^3} \cdot V^2 = p \cdot \frac{\epsilon_0 A}{z_1^3} \cdot V^2 \quad (7)$$

$$r_{\text{eff}} = \sqrt{\left( \sqrt[3]{\frac{z_1^3}{p}} - z_1 \right) \cdot r_{\text{tip}}} \quad (8)$$

The percentage factor  $p$  (e.g., for 12% percent approach:  $p$  equals 12%/100%) serves as a fitting parameter to fit the data.  $z_1$  equals  $(z + t)$  beside the nanoparticle and  $(z + d + t)$  above the nanoparticle.  $r_{\text{tip}}$  is determined by SEM measurements of the tip. In our previous works, a 0.1% approach achieved the best agreement with the experimental data.<sup>[17,18]</sup>

**Table 1.** Models for tip characterization with their  $z$ -dependence of the force calculations.

Model	$F'(z)$
Parabolic tip (12% approach)	$\sim r_{\text{tip}}/z^2$
Parabolic tip (10% approach)	$\sim 1.1544 \cdot r_{\text{tip}}/z^2$
Hudlet (only spherical contribution)	$\sim \frac{r_{\text{tip}}^2 (2z+r_{\text{tip}})}{(z^2+r_{\text{tip}}z)^2}$
Hudlet (spherical + cone contribution)	$\sim \left( \frac{r_{\text{tip}}^2 (2z+r_{\text{tip}})}{(z^2+r_{\text{tip}}z)^2} \right) - k^2 \cdot \left( \frac{1}{z+r_{\text{tip}}} - \frac{r_{\text{tip}}}{\sin(\theta_0) \cdot (z+r_{\text{tip}})^2} \right)$

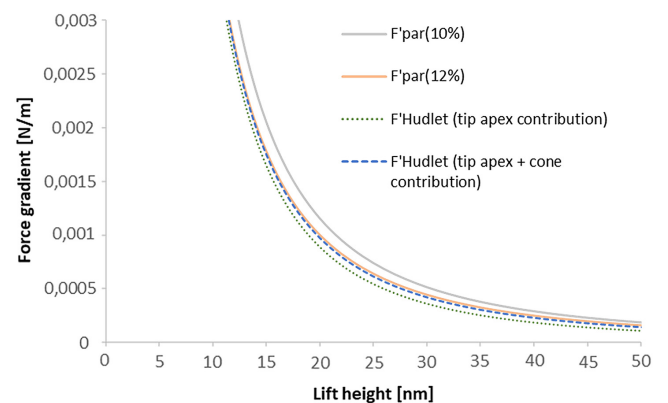


**Figure 3.** Force gradient  $F'$  as a function of lift height for the models of Table 1.

**Table 1** compares the force gradient obtained in the parabolic tip shape model and the Hudlet model and **Figure 3** shows the corresponding simulations.

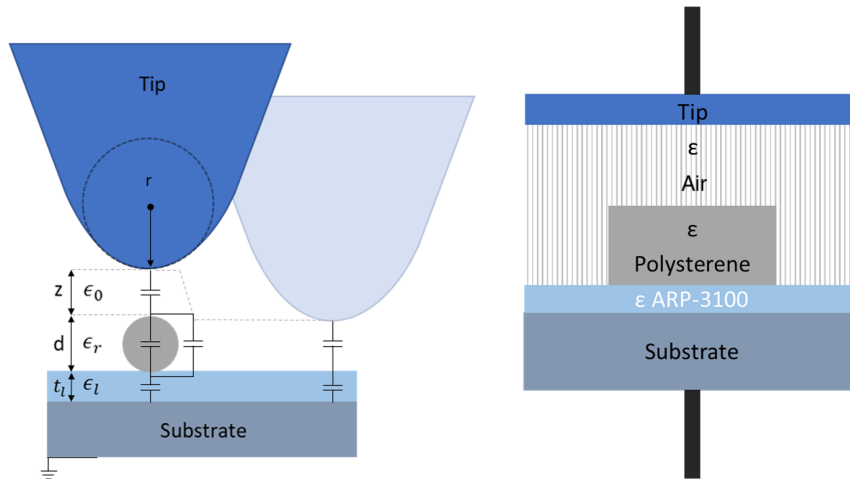


**Figure 4.** Capacitor circuit diagram considering a dielectric layer with thickness  $t_l$  and the dielectric constant of the nanoparticle.

The simulation demonstrates that the  $z$ -dependence of the parabolic tip shape model matches the  $z$ -dependence of the Hudlet model very well and can be used as a simple approach to calculate phase shifts due to capacitive coupling effects based on experimentally determined features (tip radius, parabolic form of the tip corresponding to the SEM image of our tip in Figure S1, Supporting Information).

For measurements on nanoparticles with MFM, it is necessary to use one of these models as the tip-substrate distance changes significantly above the nanoparticle and therefore the effective area of the tip-substrate area increases with increasing particle diameter.

### 2.3. Influence of the Dielectric Constant of Nanoparticles on Capacitive Coupling Effects

For small nanoparticles, the dielectric constant of the nanoparticle can be neglected due to the small ratio of the nanoparticle area to the effective area of the capacitor.

Krivcov et al. showed that for typical MFM tips and nanoparticles of 10 nm diameter, the contribution of the nanoparticle area to the effective area is below 2%.<sup>[17]</sup>

The following simulations investigate whether the dielectric constant of nanoparticles approaching the size of the tip radius has to be taken into account to calculate capacitive coupling effects. The capacitor is partially filled with the nanoparticle as shown in Figure 4. The resulting phase shift of the MFM signal can be calculated by using a capacitor circuit diagram shown in Figure 4. In this model we also include a dielectric layer with thickness  $t_l$  between the nanoparticle and the substrate as shown in Figure 1. This dielectric layer serves to minimize the capacitive coupling as reported in previous studies.<sup>[18]</sup>

Our model describing the electrostatic force between the conductive measuring tip and the substrate is based on the calculation of the capacitor circuit diagram shown in Figure 4. Tip and substrate are assumed to be the electrodes of the capacitor, which are aligned parallel to each other.

Measuring above the nanoparticles, the partially filled capacitor can be simplified as four capacitors connected in series and

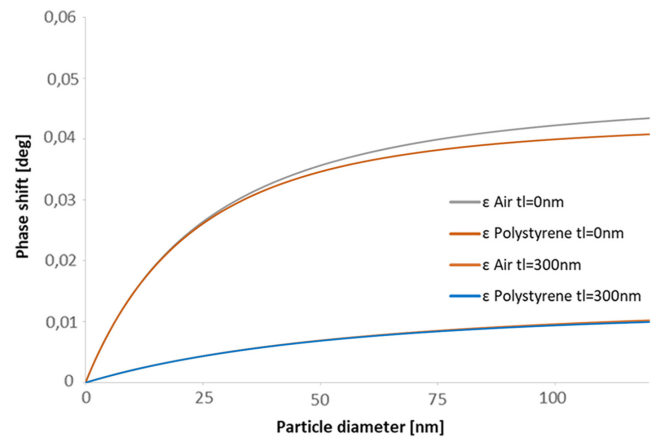


**Figure 5.** Phase shift  $\Delta\varphi_{el}$  as a function of particle diameter with  $A_{tip}$ : Parabolic model (10% approach) and  $r_{tip} = 120$  nm for two different dielectric layer thicknesses between nanoparticle and substrate.

parallel to each other (Figure 4). Measuring beside the nanoparticle, the system only consists of two capacitors connected in series. Using these equivalent circuits, the phase shift due to capacitive coupling can be calculated by

$$\Delta\varphi_{el} = -\frac{Q}{k} \epsilon_0 \cdot \left( \frac{A_{particle}}{\left(z + \frac{d}{\epsilon_{poly}} + \frac{t_l}{\epsilon_l}\right)^3} + \frac{A_{z+d+t_l} - A_{particle}}{\left(z + d + \frac{t_l}{\epsilon_l}\right)^3} - \frac{A_{z+t_l}}{\left(z + \frac{t_l}{\epsilon_l}\right)^3} \right) \cdot V_{CPD}^2 \quad (9)$$

where  $A_{particle}$  is given by  $\pi r_{particle}^2$ ,  $\epsilon_{poly}$  is the dielectric constant of the nanoparticle,  $d$  is the particle diameter,  $\epsilon_l$  is the dielectric constant of the dielectric layer with thickness  $t_l$ ,  $z$  is the lift height, and  $A$  is the effective area of the tip-substrate capacitor depending on the actual tip substrate distance,  $z + d + t_l$  measuring above the nanoparticle and  $z + t_l$  beside the nanoparticle.

Figure 5 shows the phase  $\Delta\varphi_{el}$  as a function of the particle size including the dielectric constant of the nanoparticle.

To demonstrate the influence of the dielectric constant, the calculations are compared assuming  $\epsilon = 1$  (denoted as  $\epsilon$  Air) and  $\epsilon = 2.5$  (denoted as  $\epsilon$  Polystyrene) as dielectric constant for the nanoparticle:

Calculating the phase  $\Delta\phi_{el}$  as shown in Figure 4 as a function of the particle diameter demonstrates that the dielectric constant of the nanoparticle has no significant influence on the capacitive coupling effect. This is because the volume fraction of the nanoparticle does not change significantly because as the particle diameter increases, the effective area increases as well. Introducing a dielectric layer, the topographic effect is reduced as the ratio of the distance change above the nanoparticle ( $d$ ) to the distance tip-substrate ( $t_1 + z$ ) is diminished as calculated in Figure 4 and described in previous study.<sup>[18]</sup> But, the dielectric layer also reduces the volume fraction of the nanoparticle in the tip-substrate capacitor and thus the contribution of the nanoparticle to the signal.

In general, this has the consequence that the topographic effect due to capacitive coupling makes it difficult to determine the dielectric constant of nanoparticles in interleave mode measurements such as mainly performed in EFM or MFM. Linear mode measurements performed in MFM and EFM allow the determination of the dielectric constant as there is no distance change above the nanoparticle.<sup>[12]</sup> This mode is difficult to perform on large areas due to crashes of the tip with the substrate especially while measuring nanoparticles with different heights.<sup>[17]</sup>

### 3. Results and Discussion

To investigate the influence of the dielectric constant of the polystyrene nanoparticles on MFM signals, measurements in the MFM interleave mode were performed. As the nanospheres are not loaded with magnetic nanoparticles, the signals are only due to electrostatic forces, namely capacitive coupling effects as described in Section 2.

Figure 6 shows the phase shift as a function of particle diameter for two different tip radii measured at a lift height of 50 nm.

As described in Equation (8), the capacitive coupling strongly depends on the radius of the measuring tip. Therefore, an increased radius of the tip results in larger phase shifts. The experimental data are fitted by the parabolic tip model with the tip radii determined by the SEM measurements. The only fit parameter was  $p$ , the percentage of  $F'$  taken into account (see Section 2.2.). Similar to fits in our previous works, best fits are achieved with a 0.1% approach. This reflects a rather big effective area for large tip-substrate distances.<sup>[17,18]</sup> Further investigations to explain this low value of  $p$  are necessary and ongoing.

The measurements are in accordance with the theoretical model of a parabolic tip described in Section 2.2. In this model, the effective area of the tip-substrate capacitor increases with increasing tip-substrate distance. As an increasing particle diameter leads to an enlarged tip-substrate distance, the effective area increases as well so that the dielectric constant of nanoparticles with radii approaching the size of the tip radius has no significant influence on the phase shift.

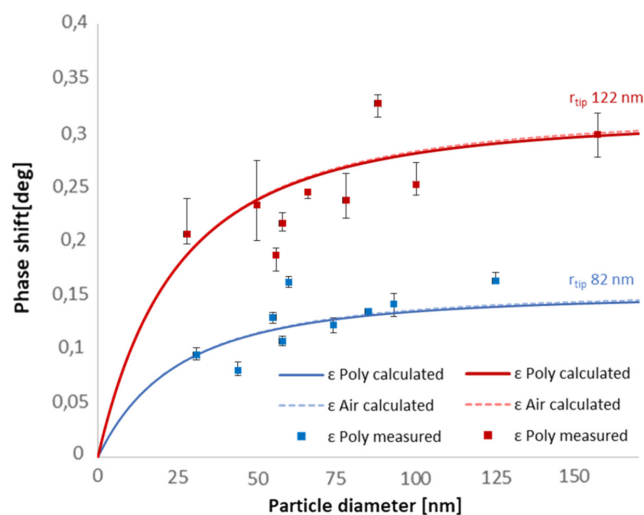


**Figure 6.** Measurements and calculations of phase shifts: tip radius  $r_{tip} = 82$  nm (blue line) and  $r_{tip} = 122.5$  nm (red line) and lift height of 50 nm. Fits were done using the parabolic model (0.1% approach) and the respective  $V_{CPD} = 0.45$  V and  $V_{CPD} = 0.6$  V (silicon substrate) using  $\epsilon$  Air = 1 and  $\epsilon$  polystyrene = 2.5.

### 4. Conclusion

In summary, we could theoretically and experimentally evaluate the influence of the dielectric constant of nanoparticles on capacitive coupling effects in interleave mode measurements in EFM and MFM. We showed that due to the distance change measuring above the nanoparticle, the effective area of the tip-substrate capacitor is correlated to the nanoparticle diameter. An increasing particle diameter leads to an enlarged effective area of the capacitor. For that reason, the volume fraction of the nanoparticle in the capacitor does not automatically increase with increasing particle diameter. Therefore, the dielectric constant of the nanoparticles has no significant impact on the capacitive coupling effect occurring in MFM and EFM measurements on nanoparticles. This effect hinders the determination of dielectric constants of nanoparticles in interleave mode measurements. In future, these investigations will help to separate the topographic cross talk from magnetic signals of nanospheres loaded with magnetic nanoparticles.

### 5. Experimental Section

Polystyrene nanoparticles were prepared through emulsification/solvent evaporation method, according to the procedure described by Musyanovych et al.<sup>[22]</sup> Briefly, 300 mg of polystyrene ( $M_w$  192 000 g mol<sup>-1</sup>, Sigma-Aldrich) were dissolved in 10 g of chloroform ( $\geq 99.8\%$ , Merck) and emulsified in 24 g of 3 wt% sodium dodecyl sulfate aqueous solution for 1 h under magnetic stirring at 1000 rpm. Afterward, the macroemulsion was sonified under ice cooling for 180 s at 70% amplitude in a pulse regime (30 s sonication, 10 s pause) using Branson 450 W and 1/4" tip. The obtained miniemulsion was transferred into the 50 mL reaction flask with a large size neck and left overnight at 40 °C for the complete evaporation of chloroform. After formulation, the nanoparticles were purified by centrifugation/redispersion in pure demineralized water and characterized. The average size of obtained nanoparticles was 127 nm (PDI 0.24) and zeta potential value corresponded to  $62 \pm 4$  mV.



Before MFM measurements, the nanoparticle samples were further diluted with ultrapure water (in a ratio of 2  $\mu$ L:10 mL) to avoid agglomeration and enhance single target measurements. Two microliter of the obtained suspension was pipetted onto a freshly cleaned silicon wafer (Siegert Wafer) and dried for 24 h under ambient conditions.

The AFM and KPFM measurements of polystyrene nanospheres were performed on a Bruker Dimension Icon Atomic Force Microscope. To calculate the capacitive coupling, it was necessary to perform KPFM measurements for each individual tip and silicon substrate to determine the work function  $V_{CPD}$  between tip and sample. Furthermore, the measurements were performed on different areas of the sample to evaluate the difference in stability of the work function. Measurements of individual nanospheres were performed in tapping mode for the first scan and in dynamical interleave mode with a lift height of 50 nm in the second scan. Thus, the topography can be measured in the first scan, whereas the second scan showed changes in the force gradient of all long-range forces acting on the tip.

Tips used in this work were ASYMFH-HM (Asylum Research) probes. Due to fluctuations in the manufacturing process of the tips, it was necessary to characterize every probe via electron microscopy (SEM) measurements as shown in Figure S1, Supporting Information. The measurements show a radius of 81 nm with a  $V_{CPD}$  value of 0.45 V for tip 1 and a radius of 122.5 nm with a  $V_{CPD}$  value of 0.6 V for tip 2.

SEM measurements were performed on a Carl Zeiss AG - SUPRA 40 using a Bruker detector, with pixel size of 600 pm to 1 nm and aperture size 41 of 60  $\mu$ m. MFM measurements were analyzed using Nanoscope software.

## Supporting Information

Supporting Information is available from the Wiley Online Library or from the author.

## Acknowledgements

The presented results are part of the ongoing InnoProm-project "TRAPP – Nanocarrier in carrier matrix for transdermal applications" co-funded by the German state Rhineland-Palatinate, the European Funds for Regional Development (EFRE), and Karl Otto Braun GmbH & Co. Kg. The authors also acknowledge Rainer Lilischkis for the support in SEM measurements.

## Conflict of Interest

The authors declare no conflict of interest.

## Keywords

capacitive coupling, dielectric constant of nanoparticles, electric force microscopy, magnetic force microscopy

Received: September 30, 2019

Revised: December 12, 2019

Published online: January 14, 2020

- [1] R. Dianoux, F. Martins, F. Marchi, C. Alandi, F. Comin, J. Chevrier, *Phys. Rev. B* **2003**, *68*, 045403.
- [2] R. I. Revilla, eprint arXiv:1601.05969 **2016**, pp. 1–11.
- [3] A. v. Valavade, K. S. Date, M. R. Press, D. C. Kothari, *Biomed. Phys. Eng. Express* **2018**, *4*, 055023.
- [4] M. Labardi, J. Barsotti, D. Prevosto, S. Capaccioli, C. M. Roland, R. Casalini, *J. Appl. Phys.* **2015**, *118*, 224104.
- [5] F. Bertorelle, C. Wilhelm, J. Roger, F. Gazeau, C. Ménager, V. Cabuil, *Langmuir* **2006**, *22*, 5385.
- [6] J. das Neves, M. M. Amiji, M. F. Bahia, B. Sarmento, *Adv. Drug Delivery Rev.* **2010**, *62*, 458.
- [7] T. M. Nocera, J. Chen, C. B. Murray, G. Agarwal, *Nanotechnology* **2012**, *23*, 495704.
- [8] R. Tietze, J. Zaloga, H. Unterweger, S. Lyer, R. P. Friedrich, C. Janko, M. Pöttler, S. Dürr, C. Alexi, *Biochem. Biophys. Res. Commun.* **2015**, *468*, 463.
- [9] S. Laurent, D. Forge, M. Port, A. Roch, C. Robic, L. Vander Elst, R. N. Muller, *Chem. Rev.* **2008**, *108*, 2064.
- [10] Q. A. Pankhurst, J. Connolly, S. K. Jones, J. Dobson, *J. Phys. D: Appl. Phys.* **2003**, *36*, 167.
- [11] H. Qiu, G. C. Qi, Y. L. Yang, C. Wang, *J. Solid State Chem.* **2008**, *181*, 1670.
- [12] T. Mélin, H. Diesinger, D. Deresmes, D. Stiévenard, *Phys. Rev. B.* **2004**, *69*, 035321.
- [13] J. Yu, J. Ahner, D. Weller, *J. Appl. Phys.* **2004**, *96*, 494.
- [14] B. I. Kim, *Rev. Sci. Instrum.* **2009**, *80*, 023702.
- [15] L. Angeloni, D. Passeri, M. Reggente, D. Mantovani, *Sci. Rep.* **2016**, *6*, 26293.
- [16] L. Angeloni, D. Passeri, M. Reggente, M. Rossi, D. Mantovani, L. Lazzaro, F. Nepi, F. de Angelis, M. Barteri, *AIP Conf. Proc.* **2015**, *1667*, 020010.
- [17] A. Krivcov, T. Junkers, H. Möbius, *J. Phys. Commun.* **2018**, *2*, 075019.
- [18] A. Krivcov, J. Ehrler, M. Fuhrmann, T. Junkers, H. Möbius, *Beilstein J. Nanotechnol.* **2019**, *10*, 1056.
- [19] E. Tevaarwerk, D. G. Keppel, P. Rugheimer, M. G. Lagally, M. A. Eriksson, *Rev. Sci. Instrum.* **2005**, *76*, 053707.
- [20] S. Belaidi, P. Girard, G. Leveque, *J. Appl. Phys.* **1997**, *81*, 1023.
- [21] S. Hudlet, M. Saint Jean, C. Guthmann, J. Berger, *Eur. Phys. J. B* **1998**, *2*, 5.
- [22] A. Musyanovych, J. Schmitz-Wienke, V. Mailänder, P. Walther, K. Landfester, *Macromol. Biosci.* **2008**, *8*, 127.